Real- and reciprocal-space attributes of band tail states

Cite as: AIP Advances **7**, 125321 (2017); https://doi.org/10.1063/1.5008521
Submitted: 06 October 2017 • Accepted: 13 December 2017 • Published Online: 21 December 2017

John F. Wager

AIP ADVANCES **7**, 125321 (2017)

Real- and reciprocal-space attributes of band tail states

John F. Wager[a]
School of EECS, Oregon State University, Corvallis, Oregon 97331-5501, USA

(Received 6 October 2017; accepted 13 December 2017; published online 21 December 2017)

Band tail states are localized electronic states existing near conduction and valence band edges. Band tail states are invariably found to exhibit an exponential distribution defined by a characteristic (Urbach) energy. To a large extent, the band tail state density of states determines the electronic performance of an amorphous semiconductor (or insulator) in terms of its mobility. Real-space assessment of a suitable density of states model for extended (delocalized) conduction or valence band states and nearby localized band tail states leads to an expression for the peak density of band tail states at the mobility edge and for the total band tail state density. Assuming a continuous density of states and its derivative with respect to energy across the mobility edge, these densities are found to depend on only two parameters – the Urbach energy and an effective mass characterizing the extended state density above the mobility edge. Reciprocal-space assessment is then employed to deduce a probability density function associated with band tail states. The full width at half maximum of the resulting Gaussian probability density function is found to be equal to the average real-space distance of separation between band tail states, as estimated from the total band tail state density. This real- and reciprocal-space insight may be useful for developing new high-performance amorphous semiconductors and for modeling their electronic properties. https://doi.org/10.1063/1.5008521

I. INTRODUCTION

Band tail states are localized electronic states existing just below the conduction band or right above the valence band. They arise as a consequence of disorder. Thermal, structural, impurity, and/or compositional disorder can all lead to the formation of band tail states.[1–4] Since amorphous semiconductors (or insulators) normally possess significantly more disorder than their crystalline counterparts, band tail states is a topic most often discussed in the literature associated with amorphous materials.[5–7] Although band tail states may originate from different types of disorder, they unfailingly display an exponential distribution defined by a characteristic (Urbach[8]) energy.

The universal nature of disorder inducing an exponential distribution of band tail states characterized by an Urbach energy is remarkable. The Urbach rule – in which optical absorption at the band edge is found to be exponential with respect to the photon energy – is observed in an extraordinarily large number of materials systems, for example, in single crystal Si,[9] GaAs,[10] CdTe,[11] and $CuInSe_{2x}Te_{2(1-x)}$,[3] microcrystalline Si,[12] polycrystalline Si,[13] and organic halide perovskites.[14] Also, the existence of exponential band tails is reported for covalent amorphous semiconductors such as amorphous hydrogenated silicon (a-Si:H),[1,2] or silicon-germanium alloys ($a\text{-}Si_xGe_{1-x}:H$),[2] as well as for ionic amorphous semiconductors such as indium gallium zinc oxide (a-IGZO),[15–19] zinc tin oxide (a-ZTO),[15] or zinc oxynitride (ZnON).[20] Although it is evident that band tail states are exponentially distributed in energy as a result of disorder, their precise atomistic nature and a clear

[a]jfw@ece.orst.edu.

explanation for why they give rise to an exponential distribution are questions that seem to have not yet been answered to everyone's satisfaction, despite the fact that these topics are well discussed in the literature.[21–31]

Given this, our investigation of band tail states will not explicitly address these unresolved questions involving the atomistic or exponential distribution nature of band tail states. Rather, we will focus on density of states issues. We begin by assuming the presence of an exponential distribution of conduction band tail states, for example, that is established by specifying two parameters, i.e., the peak conduction band tail state density, N_{TA}, and the characteristic conduction band tail state (Urbach) energy, W_{TA}; the T subscript designates that the states are band tail states and the A subscript denotes that the states are acceptor-like, i.e., negatively charged when filled and neutral when empty. We then model a semiconductor (or insulator) as possessing both localized band tail states (with an exponential distribution) and extended (or delocalized) conduction or valence band states. Localized and extended states are distinguished by their energy with respect to a mobility edge. This near-band-edge density of states picture is our launching pad.

Next, real-space assessment is accomplished. If it is assumed that the density of states and its derivative with respect to energy are continuous across the mobility edge, it is possible to derive simple expressions for the (conduction band) peak density of band tail states (N_{TA}) and for the total band tail state density (n_{TOTAL}), both of which depend on only two parameters, i.e., the Urbach energy (W_{TA}) and an effective mass for the extended states beyond the mobility edge (m_e^*). Knowing the total band tail state density (n_{TOTAL}) allows estimation of the average real space distance of separation between band tail states ($<x_{TA}>$).

Finally, reciprocal-space assessment is undertaken. A probability density function (pdf) for band tail states is derived by beginning with the exponential-in-energy distribution of band tail states, assuming that a quadratic dispersion relationship for energy in terms of wave vector holds for band tail states, and then Fourier transforming the resulting exponential relationship from wave vector or k-space to real space. The real- and reciprocal-space topics investigated in this contribution are found to be linked since, it turns out, the average real space distance between band tail states ($<x_{TA}>$) is approximately equal to the full width at half maximum of the Gaussian pdf (FWHM) for the four semiconductors considered herein (i.e., $<x_{TA}> \approx$ FWHM).

II. TOTAL BAND TAIL STATE DENSITY

The objective of this section is to derive an expression for the peak density of conduction band tail states, N_{TA}, and for the total conduction band tail state density, n_{TOTAL}. The density of states model employed herein is shown in Fig. 1. This model is similar to those used previously to account for transport in amorphous semiconductors,[32,33] or in amorphous SiO_2,[34] but with a few important differences, as pointed out below. The valence band mobility edge, E_{VME}, separates extended (delocalized) hole states, $g_V(E)$, from an exponential distribution of localized donor-like band tail states, $g_{TD}(E)$, specified by a peak density, N_{TD}, and a characteristic (Urbach) energy, W_{TD}. Similarly, the conduction band mobility edge, E_{CME}, separates extended electron states, $g_C(E)$, from an exponential distribution of localized acceptor-like band tail states, $g_{TA}(E)$, specified by a peak density, N_{TA}, and a characteristic (Urbach) energy, W_{TA}. The density of states is continuous across both mobility edges.

Before proceeding with a derivation of N_{TA} and n_{TOTAL}, a few comments about the density of states model utilized are in order. The fundamental difference between the density of states model shown in Fig. 1 and the model employed previously,[32–34] is that the valence band maximum, E_V, is now explicitly distinguished from the valence band mobility edge, E_{VME} and the conduction band minimum, E_C, is now explicitly distinguished from the conduction band mobility edge, E_{CME} Moreover, in the present model of Fig. 1, E_V is assumed to be the energy reference establishing the density of extended (delocalized) hole states, $g_V(E)$, and E_C is taken as the energy reference determining the density of extended (delocalized) electron states, $g_C(E)$. Distinguishing E_V from E_{VME} and E_C from E_{CME} is advantageous since it avoids the problem of encountering a singularity when dg_{TD}/dE is matched to dg_V/dE or dg_{TA}/dE is matched to dg_C/dE at the mobility edge. Care must be taken when comparing the present density of states model shown in Fig. 1 to the previously

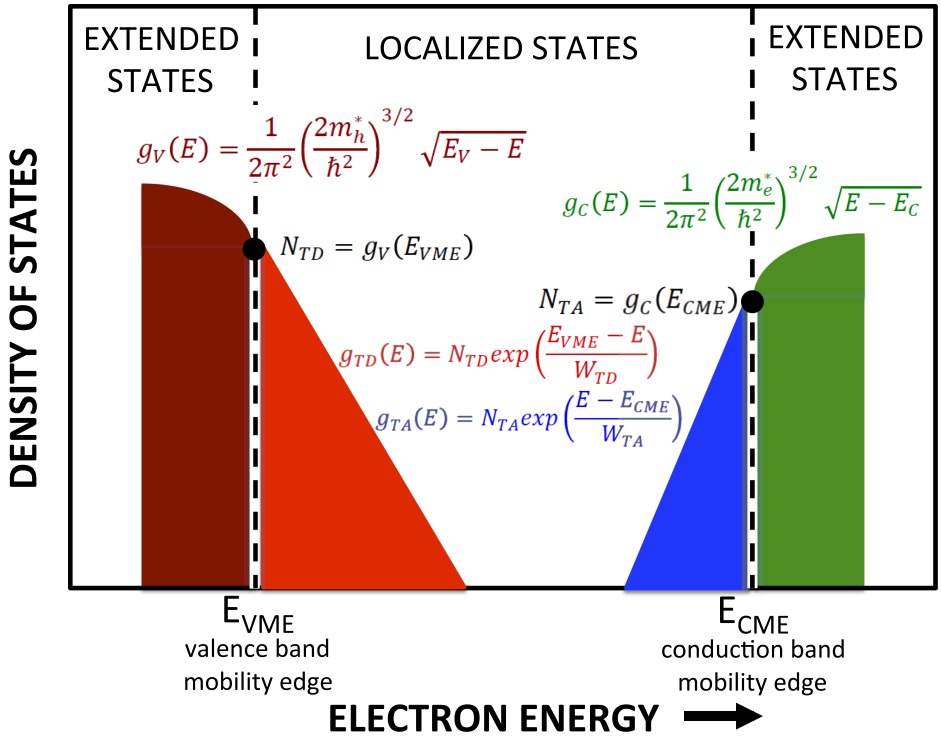

FIG. 1. Density of states model illustrating localized and extended state densities for both valence and conduction bands.

used model[32–34] since E_C and E_V were (unfortunately) previously used to denote the conduction and valence band mobility edges, respectively.

All of the subsequent discussion focuses exclusively on localized and extended states related to the conduction band. Similar considerations apply for the analogous case of localized and extended states related to the valence band.

Now proceeding with our derivation of N_{TA} and n_{TOTAL}. To ensure a smooth transition across the mobility edge, we first require that the density of states be continuous in going from localized to extended states, i.e.,

$$g_{TA}(E_{CME}) = g_C(E_{CME}) \tag{1}$$

Evaluating Eq. (1) using the expressions given in Fig. 1 leads to

$$N_{TA} = \frac{1}{2\pi^2}\left(\frac{2m_e^*}{\hbar^2}\right)^{3/2}\sqrt{E_{CME} - E_C} \tag{2}$$

where E_C is the conduction band minimum which is positioned at a lower energy than E_{CME} and established the onset of the $g_C(E)$ density of states. Next, we require that the density of states derivative with respect to energy is also continuous across the conduction band mobility edge, i.e.,

$$\frac{dg_{TA}}{dE} = \frac{dg_C}{dE} \tag{3}$$

which results in

$$\frac{N_{TA}}{W_{TA}} = \frac{1}{2\pi^2}\left(\frac{2m_e^*}{\hbar^2}\right)^{3/2}\frac{1}{2\sqrt{E_{CME} - E_C}} \tag{4}$$

Substituting N_{TA} from Eq. (2) into Eq. (4) and simplifying yields

$$E_{CME} - E_C = \frac{W_{TA}}{2} \tag{5}$$

Thus, Eq. (5) reveals that requiring continuity of the density of states and its energy derivative across the conduction band mobility edge leads to a separation between the conduction band mobility edge

and the conduction band minimum which is equal to one half of the conduction band Urbach energy. Substituting Eq. (5) into Eq. (2) results in

$$N_{TA} = \frac{1}{2\pi^2}\left(\frac{2m_e^*}{\hbar^2}\right)^{3/2}\sqrt{\frac{W_{TA}}{2}} = 4.9\times10^{21}\sqrt{W_{TA}}\left(\frac{m_e^*}{m_o}\right)^{3/2} \quad (cm^{-3}eV^{-1}) \tag{6}$$

where in the last expression W_{TA} is expressed in units of eV and m_e^*/m_o is a unitless electron effective mass associated with extended states in the conduction band. This is a key result. The peak band tail state density is a difficult quantity to estimate experimentally. Equation (6) asserts that N_{TA} assessment can be accomplished knowing only the Urbach energy and the effective mass characterizing extended band states. The density of states units associated with N_{TA}, i.e., $cm^{-3}eV^{-1}$, are likely to be unfamiliar or perhaps a bit obtuse to many readers.

A descriptive parameter with a more intuitively appealing set of units can be obtained by recognizing that $n_{TOTAL} = N_{TA}W_{TA}$ (cm^{-3}), where n_{TOTAL} is the total density of conduction band tail states.[32,33] Thus, from Eq. (6), we find that

$$n_{TOTAL} = 4.9\times10^{21}\left(W_{TA}\frac{m_e^*}{m_o}\right)^{3/2} \quad (cm^{-3}) \tag{7}$$

This result is also important. It tells us that the total amount of conduction band tail disorder present in a semiconductor or an insulator depends on the magnitude of its Urbach energy and the effective mass characterizing its extended band states. Although the volume density units of Eq. (7) are less intimidating than the density of states units of Eq. (6), certain physical comparisons are more straightforward if accomplished using a length scale, e.g., cm or nm. Such a scale is obtained by defining the average real space distance between conduction band tail states as follows

$$< x_{TA} >= 2\left(\frac{3}{4\pi\, n_{TOTAL}}\right)^{1/3} \quad (cm) \tag{8}$$

Note that $<x_{TA}>$ is equal to twice the Wigner-Seitz radius, r_s.[35] Equations (7) and (8) are employed in Section IV in a comparison of conduction band tail state trends for four selected semiconductors.

III. BAND TAIL STATES PROBABILITY DENSITY FUNCTION

The objective of this section is to derive an expression for the conduction band tail states probability density function. Begin with an expression for the density of states associated with conduction band tail states,

$$g_{TA}(E) = N_{TA}e^{\frac{E-E_{CME}}{W_{TA}}} \quad (cm^{-3}eV^{-1}) \tag{9}$$

Note that this relationship pertains when $E - E_{CME} \leq 0$, while $g_{TA}(E) = 0$ for $E - E_{CME} > 0$. Next, assume as an ansatz that the band tail state dispersion relationship is given by

$$E - E_{CME} = \frac{-\hbar^2k^2}{2m_e^*} \tag{10}$$

where $\hbar$ is the normalized Planck constant and k is the wave vector. The negative sign included in Eq. (10) can be reconciled as arising from the fact that E is smaller than E_{CME} for states below the mobility edge, or equivalently, that the wave vector is an imaginary quantity for localized, evanescent states existing below the mobility edge. Substituting Eq. (10) into Eq. (9) and dividing by N_{TA} yields

$$g_{TA}(k) = e^{\frac{-\hbar^2k^2}{2m_e^*W_{TA}}} \quad (unitless) \tag{11}$$

This is a k-space or reciprocal space density of states relationship for the conduction band tail states. Using the inverse Fourier transform defined by

$$g_{TA}(x) = \frac{1}{2\pi}\int_{-\infty}^{\infty} g_{TA}(k)\, e^{jkx}dk \tag{12}$$

allows Eq. (11) to be transformed from k-space to real space, leading to

$$g_{TA}(x) = \frac{1}{\hbar}\sqrt{\frac{m_e^* W_{TA}}{2\pi}}\, e^{\frac{-m_e^* W_{TA} x^2}{2\hbar^2}} \quad (cm^{-1}) \tag{13}$$

This is the conduction band tail states probability distribution function (pdf). Equation (11) is the corresponding characteristic function to the pdf specified in Eq. (13).[36] Note that Eq. (13) is Gaussian with a variance given by

$$\sigma^2 = \frac{\hbar^2}{m_e^* W_{TA}} \tag{14}$$

and a full width at half maximum equal to

$$FWHM = 2\sqrt{2ln2}\,\sigma \tag{15}$$

Elucidation of the meaning and utility of Eqs. (13) and (15) is best accomplished by considering specific examples, as undertaken next.

IV. ASSESSMENT OF FOUR SEMICONDUCTORS

Table I summarizes conduction band tail states trends for four semiconductors, i.e., crystalline gallium arsenide (c-GaAs), crystalline silicon (c-Si), amorphous indium gallium zinc oxide (a-IGZO), and amorphous hydrogenated silicon (a-Si:H).[32,33] The optical absorption Urbach energy for c-GaAs and c-Si are reported to be 5.9 meV[10] and 8.5 ± 1.0 meV,[9] respectively. However, these optical absorption Urbach energies are determined by valence band tail states, which are wider than their corresponding conduction band tail states. We consider our W_{TA} ~3 and ~4 meV estimates for c-GaAs and c-Si, respectively, to be crude approximations. More likely, W_{TA}(c-GaAs) = 3 ± 3 meV and W_{TA}(c-Si) = 4 ± 4 meV. Note that we include a second entry of W_{TA} ~0.3 and ~0.5 meV for c-GaAs and c-Si, respectively, in Table I. These alternative Urbach energy estimates are considered later in the context of the characteristic distance and time comparisons presented in Table II. Even though our estimates of W_{TA} for c-GaAs and c-Si are imprecise, the main point here is that W_{TA} for a crystalline semiconductor is much smaller than it is for an amorphous semiconductor. As shown in the following discussion, this has important consequences.

Equation (6) is used to calculate N_{TA} in Table I. Our Table I estimate of N_{TA}(a-IGZO) = 1.1 × 10^{20} $cm^{-3}eV^{-1}$ is slightly larger than the 1.55 × 10^{20} $cm^{-3}eV^{-1}$ value reported by Fung et al.,[16]

TABLE I. A conduction band tail states comparison of four semiconductors.

Semiconductor	m_e^* (unitless)	W_{TA} (meV)	N_{TA} ($cm^{-3}eV^{-1}$)	n_{TOTAL} (cm^{-3})	$<x_{TA}>$ (nm)	FWHM (nm)
c-GaAs	0.063	~3	4.2×10^{18}	1.3×10^{16}	53	47
		~0.3	1.3×10^{18}	4.0×10^{14}	170	150
c-Si	0.26	~4	4.1×10^{19}	1.6×10^{17}	23	20
		~0.5	1.5×10^{19}	7.3×10^{15}	64	57
a-IGZO	0.34	13	1.1×10^{20}	1.4×10^{18}	11	8.5
a-Si:H	0.4	33	2.3×10^{20}	7.4×10^{18}	6.4	5.7

TABLE II. A characteristic distance and time comparison of four semiconductors.

Semiconductor	μ_i or μ_0 ($cm^2V^{-1}s^{-1}$)	λ_{mfp} (nm)	$<x_{TA}>$ (nm)	$<\tau_m>$ (fs)	$\hbar/6W_{TA}$ (fs)
c-GaAs	8000	133	53 (W_{TA} = 3 meV)	290	37 (W_{TA} = 3 meV)
			170 (W_{TA} = 0.3 meV)		370 (W_{TA} = 0.3 meV)
c-Si	1450	49	23 (W_{TA} = 4 meV)	215	28 (W_{TA} = 4 meV)
			64 (W_{TA} = 0.5 meV)		220 (W_{TA} = 0.5 meV)
a-IGZO	22	0.85	11	4.3	8.5
a-Si:H	15	0.61	6.4	3.3	3.3

but is somewhat larger than 4.23×10^{19} $cm^{-3}eV^{-1}$, as given by Yu et al.[18] Also, our estimate of N_{TA}(a-Si:H) = 2.3×10^{20} $cm^{-3}eV^{-1}$ is at the lower end of the range of values reported in the literature, i.e., 2×10^{20} to 5×10^{22} $cm^{-3}eV^{-1}$.[37] As mentioned previously, it is difficult to unambiguously determine an accurate value for N_{TA}. We are aware of no prior estimates of N_{TA} for either c-GaAs or c-Si.

Figure 2 is a plot of density of states versus energy near the conduction band for the four semiconductors under consideration. The plots shown in Fig. 2 are generated using the density of states expressions included in Fig. 2 for $g_C(E)$ and $g_{TA}(E)$, and using the values for m_e^*, W_{TA}, and N_{TA} that are collected in Table I. In all four cases, the density of states is continuous across the mobility edge. The density of states magnitude trend of Fig. 2 in which a-Si:H > a-IGZO > c-Si > c-GaAs is consistent with that the trend established by N_{TA} in Table I.

Returning to our discussion of Table I, once W_{TA} and N_{TA} are known, n_{TOTAL} can be calculated using Eq. (7). The resulting estimates for n_{TOTAL} that are collected in Table I are quite intriguing. The overall trend is that n_{TOTAL}(a-Si:H) > n_{TOTAL}(a-IGZO) > n_{TOTAL}(c-Si) > n_{TOTAL}(c-GaAs). Defining n_{TOTAL} allows this trend to be quantified. Thus, according to the n_{TOTAL} estimates included in Table I, a-Si:H possesses approximately 5, 44 (1,000, if W_{TA}(c-Si) = 0.5 meV), or 570 (18,500, if W_{TA}(c-GaAs) = 0.3 meV) times more disorder-induced conduction band tail states than a-IGZO, c-Si, or c-GaAs, respectively. Another way to quantify conduction band tail state disorder is to formulate it on a parts-per-million (ppm) basis by defining $n_{ppm} = n_{TOTAL}/n_{ATOMIC} \times 10^6$, where n_{ATOMIC} is atomic concentration. This leads to $n_{ppm} \approx 0.3$ (0.009, if W_{TA}(c-GaAs) = 0.3 meV), 3 (0.15, if W_{TA}(c-Si) = 0.5 meV), 17, 150 ppm if $n_{ATOMIC} = 4.43$, 5.02, 8.2, or 4.9×10^{22} cm^{-3} for c-GaAs, c-Si, a-IGZO, or a-Si:H, respectively. This ppm approach indicates that the extent of disorder is modest from the perspective of atomic density, even for the most disordered semiconductor considered, i.e., a-Si:H. However, from the perspective of impurity doping, a-Si:H would be classified as a strongly disordered semiconductor given that n_{TOTAL}(a-Si:H) = 7.4×10^{18} cm^{-3}, a density corresponding to degenerate doping for most semiconductors.

The last two columns of Table I provide us with yet one more approach for quantifying conduction band tail state disorder. Note that $<x_{TA}> \approx$ FWHM. This establishes that the average real space distance between conduction band tail states, i.e., $<x_{TA}>$, is essentially equivalent to the full width at half maximum of the conduction band tail state pdf, i.e., FWHM. This correspondence between $<x_{TA}>$ and FWHM is both surprising and encouraging. It suggests that we have arrived at a unique length-scale estimator of conduction band tail state disorder after following two distinctly different paths of inquiry involving real space or reciprocal space.

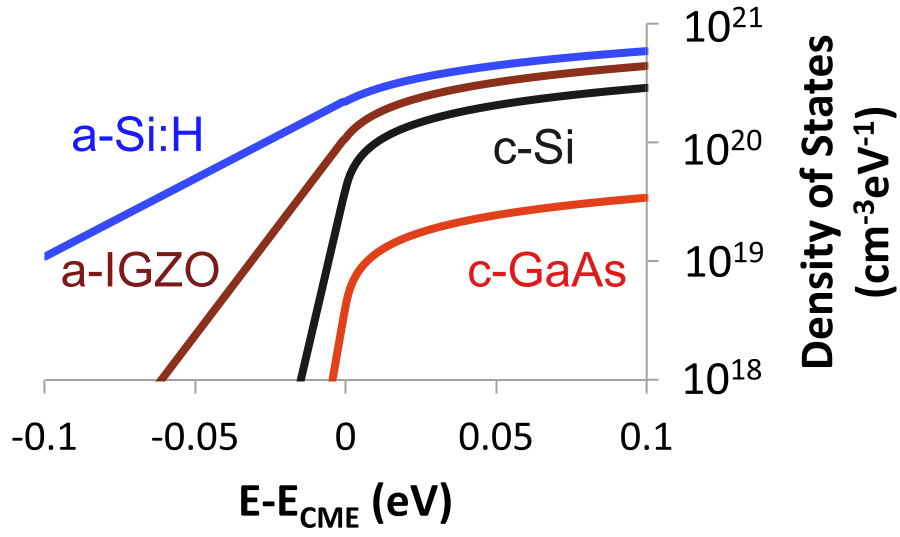

FIG. 2. Near-conduction band density of states plots for four semiconductors using values for m_e^*, W_{TA}, and N_{TA} as given in Table I. W_{TA}(c-GaAs) = 3 meV and W_{TA}(c-Si) = 4 meV for this simulation.

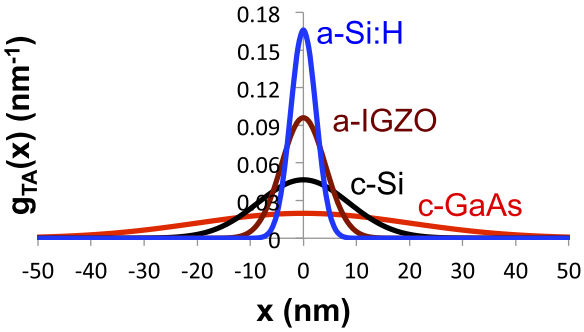

FIG. 3. Conduction band tail state probability density function (pdf) as a function of distance for four semiconductors. W_{TA}(c-GaAs) = 3 meV and W_{TA}(c-Si) = 4 meV for this simulation.

To further explore the meaning of the FWHM entry to Table I, consider Fig. 3 in which the conduction band tail states pdf, $g_{TA}(x)$, is plotted as a function of distance, x, using Eq. (13) to calculate $g_{TA}(x)$. Since the conduction band tail states for c-GaAs (especially) and for c-Si (also) are hyper-abrupt in energy or wave-vector space, they are spread out in real space, as clearly evident from Fig. 3. In contrast, since conduction band tail states for a-Si:H (especially) and for a-IGZO (also) are relatively broad in energy or wave-vector space, they are fairly abrupt in real space. This trend of spreading in one space due to compression in another space is a well-known feature of a Fourier transform pair.[36]

This spreading-compression Fourier transform tendency is once again illustrated by comparing the pdf curves of Fig. 3 to the characteristic function plots of Fig. 4. The characteristic function of a strongly-ordered, crystalline semiconductor such as c-GaAs (especially) or c-Si (also) is compressed in reciprocal space (Fig. 4), but is dispersed in real space (Fig. 3). In contrast, for a disordered semiconductor such as a-Si:H (especially) or a-IGZO (also), the characteristic function is more spread out in k-space (Fig. 4), while it is compressed in real space (Fig. 3).

As asserted previously, $g_{TA}(x)$ is a pdf. Perhaps the strongest reason for identifying $g_{TA}(x)$ as a pdf for conduction band tail states is the following observation. Recognize that $g_{TA}(k)$ is the Fourier transform of $g_{TA}(x)$, i.e.,

$$g_{TA}(k) = \int_{-\infty}^{\infty} g_{TA}(x)\, e^{-jkx} dx \tag{16}$$

Evaluating Eq. (16) at k = 0 results in

$$g_{TA}(k=0) = \int_{-\infty}^{\infty} g_{TA}(x)\, dx = 1 \tag{17}$$

This equation demonstrates two important properties of a pdf:[36] (i) the characteristic function of a pdf evaluated at zero, i.e., the left side of Eq. (17), is equal to 1 (as shown in Fig. 4), and (ii) the

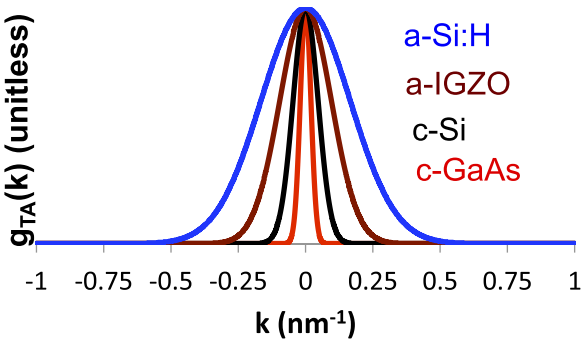

FIG. 4. Conduction band tail state characteristic function as a function of wave vector, k, for four semiconductors. Note that g_{TA}(k=0) = 1. W_{TA}(c-GaAs) = 3 meV and W_{TA}(c-Si) = 4 meV for this simulation.

integral of a pdf over all space, i.e., the middle integral shown in Eq. (17), is equal to 1. Thus, $g_{TA}(x)$ is normalized, as required for a pdf.

Having established that $g_{TA}(x)$ is a conduction band tail states pdf, how do we interpret a $g_{TA}(x)$ plot, such as those shown in Fig. 3? Begin by recognizing that the x = 0 origin of a $g_{TA}(x)$ plot corresponds to the position in real space of one individual conduction band tail state out of the n_{TOTAL} available (per unit volume). On average, the nearest conduction band tail state is located (in real space) at a distance of ~ $<x_{TA}>$ nm away from the x = 0 origin. However, it is important to recognize that this ~ $<x_{TA}>$ distance of separation is a random variable. This means that the real space in which this conduction band tail state exists is stochastic or probabilistic in nature, as is its corresponding Fourier transform reciprocal space. This is distinctly different than the deterministic perspective normally adopted in discussions of real versus reciprocal space. Note that for 'normal' reciprocal space, the wave vector, k, is a real quantity corresponding to a propagating state. In contrast, k is an imaginary quantity corresponding to a decaying, evanescent, localized state for the reciprocal space associated with conduction band tail states.

When a $g_{TA}(x)$ plot is generated, we have no idea whether the conduction band tail state of interest is obtained from a weakly localized band tail state near the mobility edge (orange state of Fig. 5) or from a strongly localized band tail state remotely positioned in energy from the mobility edge (red state of Fig. 5). However, $g_{TA}(x)$ must account for the physical positioning of both of these states, as well as of all other conduction band tail states, in a probabilistic manner. The probability of finding a conduction band tail state located between a and b (in x), is given by

$$P(a \le x \le b) = \int_a^b g_{TA}(x)\,dx \tag{18}$$

This property is another consequence of identifying $g_{TA}(x)$ as a pdf for conduction band tail states. If it is assumed that a = -1 nm and b = 1 nm, then P(-1 nm ≤ x ≤ 1 nm) ≈ 4, 9, 19, or 32% for c-GaAs, c-Si, a-IGZO, or a-Si:H, respectively. Visualizing these trends is possible with the aid of Fig. 3.

Table II presents a characteristic distance and time comparison for the same four semiconductors that are included in Table I. From the intrinsic mobility, μ_i, of a crystalline semiconductor or

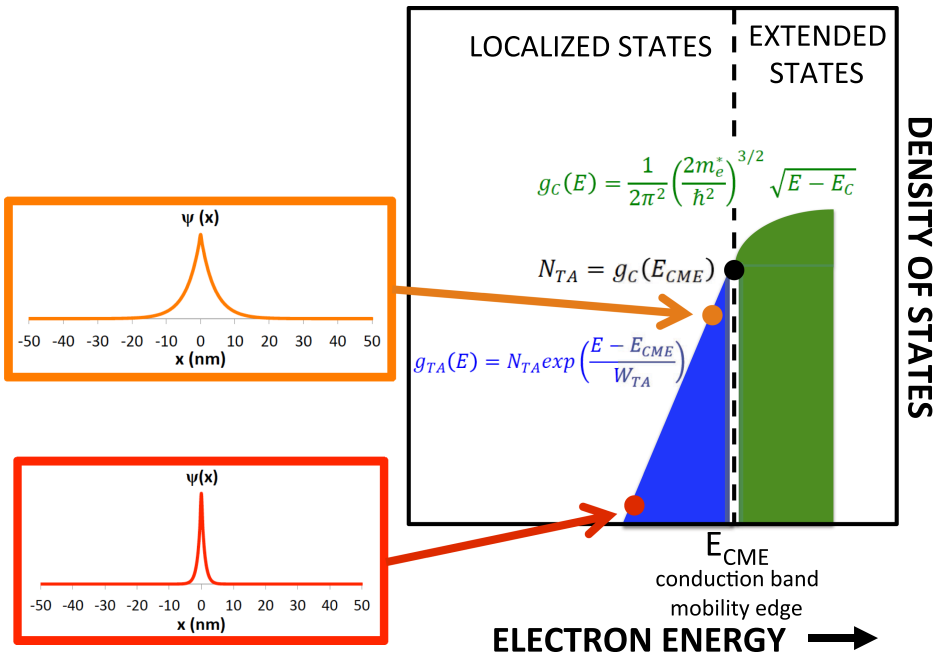

FIG. 5. Examples of gradually (orange) and abruptly (red) decaying wave functions for localized conduction band tail states.

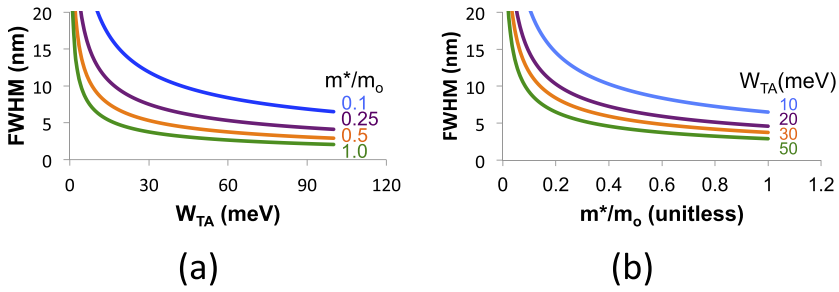

FIG. 6. Full width at half maximum (FWHM) for the conduction band tail state probability density function [$g_{TA}(x)$] versus (a) conduction band Urbach energy (W_{TA}) and (b) relative effective mass (m^*/m_o).

from the diffusive mobility, μ_0, of an amorphous semiconductor, the mean free path, λ_{mfp}, and the average momentum relaxation time, $<\tau_m>$, may be estimated.[32,34] λ_{mfp} and $<\tau_m>$ are useful electron transport parameters. The last entry in Table II, i.e., $\hbar/6W_{TA}$, is a scattering time for the Urbach energy-limited diffusive mobility. To clarify, the Urbach energy-limited diffusive mobility is given by $\mu_0 = q\hbar/6m^*W_{TA}$.[34] Recognizing $\hbar/6W_{TA}$ as a scattering time that we (loosely) denote as $<\tau_m>$ leads to $\mu_0 = q<\tau_m>/m^*$, which is the standard defining equation for mobility.

Returning to the distance and time comparisons of Table II, the amorphous semiconductor trends in which λ_{mfp} is less than $<x_{TA}>$ and $<\tau_m>$ is less than or equal to $\hbar/6W_{TA}$ make sense physically. [Note that $<\tau_m>$ for a-IGZO is estimated using the temperature-limited diffusive mobility given by $\mu_0 = q\hbar/6m^*k_BT$.[34]] In contrast, the W_{TA}(c-GaAs) = 3 meV and W_{TA}(c-Si) = 4 meV crystalline semiconductor trends in which λ_{mfp} is greater than $<x_{TA}>$ and $<\tau_m>$ is greater than $\hbar/6W_{TA}$ are puzzling. Why would these amorphous transport parameters $<x_{TA}>$ and $\hbar/6W_{TA}$ be so small (and, hence, of dominant importance) compared to λ_{mfp} and $<\tau_m>$, respectively, for a crystalline semiconductor in which disorder is such a weak effect? This problem goes away if W_{TA}(c-GaAs) = 0.3 meV and W_{TA}(c-Si) = 0.5 meV since λ_{mfp} is less than $<x_{TA}>$ and $<\tau_m>$ is less than $\hbar/6W_{TA}$. This suggests that the 0.3 and 0.5 meV Urbach energy estimates for c-GaAs and c-Si may be more accurate. In summary, we can conclude that the crystalline Urbach energies are small and are bounded as W_{TA}(c-GaAs) = 3 ± 3 meV and W_{TA}(c-Si) = 4 ± 4 meV. However, it is impossible to deduce the conduction band tail state Urbach energy for c-GaAs or c-Si with more precision.

As mentioned previously and as evident from an assessment of Eqs. (14) and (15), FWHM for $g_{TA}(x)$ is determined by two parameters, W_{TA} and m^*/m_o. FWHM is an important quantity since it is essentially equivalent to the mean real space separation distance between conduction band tail states, i.e., FWHM ≈ $<x_{TA}>$. Thus, trends in FWHM with respect to W_{TA} and m^*/m_o are of interest and are plotted in Fig. 6 over expected ranges of W_{TA} and m^*/m_o. Only crystalline materials with relatively small effective masses and Urbach energies are likely have FWHM > ~10 nm. The effective mass and Urbach energy of most amorphous semiconductors and insulators are larger, such that ~4 nm < FWHM < ~8 nm.

V. CONCLUSIONS

Assessment of the physics of conduction band tail states reveals the existence of a reciprocal space in which wave vectors are imaginary since they correspond to decaying, evanescent, localized states, rather than the propagating states of 'normal' k-space. Fourier transforming from this imaginary, reciprocal conduction band tail states space back into real physical space leads to the emergence of a probability density function describing the stochastic nature of the real space separation distance between conduction band tail states. The amount of disorder present in a given semiconductor or insulator can be estimated from its Urbach energy and its effective mass characterizing extended states above the conduction band mobility edge. Similar considerations apply to the physics of valence band tail states.

ACKNOWLEDGMENTS

I am grateful to the anonymous reviewer of this manuscript for pointing out that the existence of a singularity in the matched energy derivatives of localized and extended states at the mobility edge could be avoided by simply distinguishing between a band extremum and its mobility edge.

[1] G. D. Cody, T. Tiedje, B. Abeles, B. Brooks, and Y. Goldstein, Phys. Rev. Lett. **47**, 1480 (1981).
[2] S. Aljishi, J. D. Cohen, S. Jin, and L. Ley, Phys. Rev. Lett. **64**, 2811 (1990).
[3] S. M. Wasim, C. Rincón, G. Marín, P. Bocaranda, E. Hernández, I. Bonalde, and E. Medina, Phys. Rev. B **64**, 195101 (2001).
[4] P. Van Mieghem, Rev. Mod. Phys. **64**, 755 (1992).
[5] N. F. Mott and E. A. Davis, *Electronic Processes in Non-Crystalline Materials*, 2nd Ed. (Clarendon Press, Oxford, 1979).
[6] S. R. Elliot, *Physics of Amorphous Materials* (Longman Group Ltd., London, 1984).
[7] R. A. Street, *Hydrogenated Amorphous Silicon* (Cambridge University Press, Cambridge, 1991).
[8] F. Urbach, Phys. Rev. **92**, 1324 (1953).
[9] C. H. Grein and S. John, Phys. Rev. B **39**, 1140 (1989).
[10] M. Beaudoin, A. J. G. DeVries, S. R. Johnson, H. Laman, and T. Tiedje, Appl. Phys. Lett. **70**, 3540 (1997).
[11] E. Belas, Š. Uxa, R. Grill, P. Hlídek, L. Šedivý, and M. Bugár, J. Appl. Phys. **116**, 103521 (2014).
[12] R. Brüggemann, J. Appl. Phys. **92**, 2540 (2002).
[13] J. Werner and M. Peisl, Phys. Rev. B **31**, 6881 (1985).
[14] S. De Wolf, J. Holovsky, S.-J. Moon, P. Löper, B. Niesen, M. Lendinsky, F.-J. Haug, J.-H. Yum, and C. Ballif, J. Phys. Chem. Lett. **5**, 1035 (2014).
[15] P. T. Erslev, E. S. Sundholm, R. E. Presley, D. Hong, J. F. Wager, and J. D. Cohen, Appl. Phys. Lett. **95**, 192115 (2009).
[16] T.-C. Fung, C.-S. Chuang, C. Chen, K. Abe, R. Cottle, M. Townsend, H. Kumomi, and J. Kanicki, J. Appl. Phys. **106**, 084511 (2009).
[17] T. Kamiya, K. Nomura, and H. Hosono, Sci. Tech. Adv. Mater. **11**, 044305 (2010).
[18] E. K.-H. Yu, S. Jun, D. H. Kim, and J. Kanicki, J. Appl. Phys. **116**, 154505 (2014).
[19] A. de Jamblinne de Meux, G. Pourtois, J. Genoe, and P. Heremans, J. Phys. D **48**, 435104 (2015).
[20] S. Lee, A. Nathan, Y. Ye, Y. Guo, and J. Robertson, Sci. Rep. **5**, 13467 (2015).
[21] J. D. Dow and D. Redfield, Phys. Rev. B **5**, 594 (1972).
[22] C. Soukoulis and M. H. Cohen, J. Non-Cryst. Solids **66**, 279 (1984).
[23] C. Soukoulis, M. H. Cohen, and E. C. Economou, Phys. Rev. Lett. **53**, 616 (1984).
[24] W. Sritakool, V. Sa-yakanit, and H. R. Glyde, Phys. Rev. Lett. **33**, 1199 (1986).
[25] D. Monroe and M. A. Kastner, Phys. Rev. Lett. **33**, 1881 (1986).
[26] S. John, C. Soukoulis, Y. Ye, M. H. Cohen, and E. N. Economou, Phys. Rev. Lett. **57**, 1777 (1986).
[27] N. Becalis, E. N. Economou, and M. H. Cohen, Phys. Rev. B **37**, 2114 (1988).
[28] M. H. Cohen, M. Y. Chou, E. N. Economou, S. John, and C. Soukoulis, IBM J. Res. Develop. **32**, 82 (1988).
[29] M. Silver, L. Pautmeier, and H. Bässler, Solid State Commun. **72**, 177 (1989).
[30] J. Dong and D. A. Drabold, Phys. Rev. Lett. **80**, 1928 (1998).
[31] Y. Pan, F. Inman, M. Zhang, and D. A. Drabold, Phys. Rev. Lett. **100**, 206403 (2008).
[32] K. A. Stewart, B.-S. Yeh, and J. F. Wager, J. Non-Cryst. Solids **432B**, 196 (2016); **455**, 102 (2017).
[33] K. A. Stewart and J. F. Wager, J. Soc. Inf. Disp. **24**, 386 (2016).
[34] J. F. Wager, J. Non-Cryst. Solids **459**, 111 (2017).
[35] L. A. Girifalco, *Statistical Mechanics of Solids* (Oxford University Press, Oxford, 2000), p. 125.
[36] A. Papoulis, *Probability, Random Variables, and Stochastic Processes*, 2nd Ed. (McGraw-Hill, New York, 1984).
[37] S. D. Brotherton, *Introduction to Thin Film Transistors* (Springer, Heidelberg, 2013).